euspen's 19th International Conference & Exhibition, Bilbao, ES, June 2019
www.euspen.eu

Adaptive tracking control of dual position loops drive using active-disturbance-rejection control

Baozhu Xue[1], Chengyong Zhang[1] ,Longfei Zhang[1], Miannuo Chen[1], Yaolong Chen[1]

[1]*State Key Laboratory for Manufacturing Systems Engineering, Xi'an Jiaotong University, No.99, Yanxiang Road, Xi'an, Shaanxi,710054, China*

xbz1161211843@stu.xjtu.edu.cn

Abstract

To eliminate the influence of the internal and external disturbance, a novel active-disturbance-rejection controller (ADRC) for dual position loops feed-drive system has been proposed in this paper. This controller is based on the disturbance-rejection tracking control (DRTC) and proportion-integration-differentiation (PID) control. The controller adopts a dual position loops feedback control scheme which is different from the traditional feed system with position loop and speed loop. The motor rotation angle position is used in the inner loop as the feedback signal to reduce the influence of differential error, noise amplification and filtering delay. The closed-loop control of the whole system is realized in the outer loop through the feedback of the load position. Both of the position loops have the position controller and the state observer. For the dual loops of motor and load position feedback, in order to obtain a high disturbance-rejection capability and robustness, the linear extended state observer (LESO) is used to online estimate and compensate the total disturbance, including parameter perturbations, unmodeled dynamics and other disturbances. On the base of the real-time compensation of the total disturbance, according to the error between input signal and feedback signal, and its differential, the linear feedback rate is decided by the controller to obtain higher control bandwidth. In addition, the control performance of the controller can be further improved by feedforward of speed. Comparative simulation and experimental results indicate that the presented active-disturbance-rejection controller has better tracking performance and robustness against the disturbances compared with the P-PI (proportional position controller and proportional-integral speed controller) control method. Moreover, the controller has the advantages of simple algorithm, clear physical meaning of control parameters, easy debugging and it is basically independent of accurate mathematical model of feed system.

Active-disturbance-rejection controller, dual position loops, extended state observer, speed feedforward.

1. Introduction

Because of the high stiffness, high transmission accuracy, and low sensitivity to variations in cutting force and workpiece mass, ball screw drive feed systems are widely used in modern computer numerical control (CNC) machine tools. However, the limited stiffness of the coupling, the ball screw and the support bearing results in a lower first order resonant frequency. When the parameters of the controller are set incorrectly, or the worktable is subjected to external disturbances, the feed system will generate undesired vibrations, which will affect the machining quality of the workpiece. In addition, with the increase in production efficiency requirements, high-speed CNC machine tools have been widely used, but large amplitude, high-frequency wide driving force, inertial force, cutting force of the high-speed CNC machine tools will stimulate significant vibration of the mechanical system [1-3].

Current feed system control is mainly cascade P-PI control (proportional position control and proportional-integral speed control), which is simple, easy of tuning and practical effective [4]. The speed loop achieves speed feedback via an angle encoder on the motor side. The position loop achieves semi-closed loop position control via an angle encoder or full closed loop position control via a linear encoder at the worktable. However, since the cascade control is completely independent of the mathematical model of ball screw system, and the system is nonlinear with disturbances [5], the cascade P-PI control cannot meet the requirement of high velocity and good performance. The control bandwidth is limited by the first-order resonant frequency of the feed system [6, 7], which will deteriorate the trajectory tracking accuracy.

In practical industrial applications, disturbances including unmodeled dynamics, variable parameter, friction and cutting force, will inevitable influence the control performance of the ball screw feed system. The ability of disturbance rejection is a crucial aspect to estimate control strategies. Compared to the limited ability of traditional cascade P-PI controller, many more advanced controls methods have been proposed, which could suppress the disturbances more effectively [8-12]. In 1987, Ohnishi [5] proposed the disturbance-observer (DOB), which could online estimate and compensate the disturbances and has been widely used in many control fields. The basic idea of DOB is to estimate and compensate the discrepancy between the plant and the model, as well as the external disturbances, forcing the actual system to like nominal one [13]. Elfizy A et al. [6], Yan M et al. [7] and Kempf C et al. [12] used DOB to evaluate and compensate the disturbances, and proposed composite control strategies to realize the high-precision tracking performance. In addition, as the core of the ADRC, the extended state observer (ESO) was widely applied in the field of disturbance rejection, which regarded the internal and external disturbances as a generalized disturbance [14,18]. The control strategy called active-disturbance-rejection-control (ADRC) integrated the advantages of the PID and DOB in industrial control [15-22].

Therefore, a novel ADRC for dual position loops feed-drive system has been proposed in this paper. This control strategy uses ESO to estimate and compensate the total disturbance, including internal and external disturbances. And speed feedforward was applied to further improve the control performance.

2. Modelling of the ball screw feed system

In this paper, a ball screw feed drive system (as shown in Figure 1) is taken as the object of study, which includes a servomotor, a ball screw pair, a coupling, bearings, a slide table and a workpiece. Two pairs of the angular contact ball bearings are used to support the screw shaft. The torque T generated by motor is transmitted to the slide table via coupling and the ball screw pair. This study is aimed at achieve the high-precision control by the motor torque T and the disturbance d. The model of the ball screw feed system can be seen as a double-input and double-output model. The equivalent force F_m generated by the torque T and the external disturbance F_d are the inputs of the feed system, while the equivalent linear displacement x_m of the motor angular rotation and the linear displacement x_l of the workpiece are seen as the outputs. Therefore, the model of the ball screw feed system can be regarded as

$$\begin{bmatrix} x_m(s) \\ x_l(s) \end{bmatrix} = \begin{bmatrix} G_{mm}(s) & G_{dm}(s) \\ G_{ml}(s) & G_{dl}(s) \end{bmatrix} \begin{bmatrix} F_m(s) \\ F_d(s) \end{bmatrix} \tag{1}$$

Where $G_{mm}(s)$ is the transfer function from F_m to x_m, and $G_{ml}(s)$, $G_{dm}(s)$, $G_{dl}(s)$ are the transfer functions from F_m to x_l, F_d to x_m, F_d to x_l, respectively. Moreover, $G_{mm}(s)$ and $G_{ml}(s)$ indicate the effect of tracking performance of the system, $G_{dm}(s)$ and $G_{dl}(s)$ indicate the effect of external disturbances. When it is regarded as a rigid-body with flexible modes, $G_{mm}(s)$ and $G_{ml}(s)$ can be

$$G_{mm}(s) = \frac{x_m(s)}{F_m(s)} = \frac{1}{(ms+B)s} + \sum_{i=1}^{n} \frac{\alpha_{1i}s + \beta_{1i}}{s^2 + 2\zeta\omega_{ni}s + \omega_{ni}^2} \tag{2}$$

$$G_{ml}(s) = \frac{x_l(s)}{F_m(s)} = \frac{1}{(ms+B)s} + \sum_{i=1}^{n} \frac{\alpha_{2i}s + \beta_{2i}}{s^2 + 2\zeta\omega_{ni}s + \omega_{ni}^2} \tag{3}$$

Where m is the sum of the equivalent mass of motor m_m and load m_l(m $= m_m + m_l$), while B is the viscous damping. ζ and ω_{ni} are the damping ratio and the natural frequency of the flexible mode respectively, while α and β are the residual modes. Moreover, the model is seen as a two-mass model, and the functions are

$$G_{mm}(s) = \frac{m_l s^2 + Cs + K}{s^2\left[m_m m_l s^2 + (m_m + m_l)Cs + (m_m + m_l)K\right]} \tag{4}$$

$$G_{ml}(s) = \frac{Cs + K}{s^2\left[m_m m_l s^2 + (m_m + m_l)Cs + (m_m + m_l)K\right]} \tag{5}$$

Where C is the equivalent damping, and K indicates the equivalent stiffness.

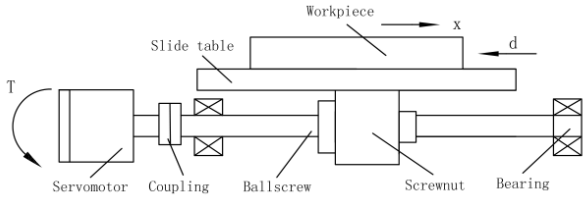

Figure 1. Schematic of the ball screw feed drive system.

3. Controller design

Figure 2 shows the scheme of the active-disturbance-rejection controller. In this system there are mainly four parts: (1) load position controller, (2) load position state observer, (3) motor position controller, (4) motor position state observer.

3.1. Motor position controller design

It can be analyzed from dynamic characteristic that the model is dominated by the rigid body mode, therefore $G_{mm}(s)$ can be expressed as

$$\ddot{y} = (b_0 + \Delta b)u + f_h + \omega + f_u = f_t + b_0 u \tag{6}$$

Where $y = x_m$, $u = F_m$, $b = b_0 + \Delta b$, while f_h and f_u represent the modeled high frequency dynamics and unmodeled dynamics respectively. And f_t represents the total disturbance, including unmodeled dynamics and external disturbances. If $x_1 = y,\ x_2 = \dot{y},\ x_3 = f_t,\ h = \dot{f}_t$. then (6) can be rewritten as

$$\begin{cases} \dot{x}_1 = x_2 \\ \dot{x}_2 = x_3 + b_0 u \\ \dot{x}_3 = h \\ y = x_1 \end{cases} \tag{7}$$

Through the linear-extended-state-observer (LESO), the evaluation values of the motor equivalent linear position Z_{m1}, the motor equivalent linear speed Z_{m2}, and the total disturbance of motor position loop Z_{m3} can be obtained by using the input of the motor control u and the motor equivalent linear position x_m

$$\begin{cases} \dot{Z}_{m1} = Z_{m2} + \beta_{m1}(x_m - Z_{m1}) \\ \dot{Z}_{m2} = Z_{m3} + \beta_{m2}(x_m - Z_{m1}) + b_{m0}u \\ \dot{Z}_{m3} = \beta_{m3}(x_m - Z_{m1}) \end{cases} \tag{8}$$

Where b_{m0} is the control gain in motor position loop, β_{m1}, β_{m2}, β_{m3} represent the gains of the observer. And the gains can be chosen as $\beta_{m1} = 3\omega_{m0}, \beta_{m2} = 3\omega_{m0}^2, \beta_{m3} = \omega_{m0}^3$. ω_{m0} is the bandwidth of the state observer. A well-tuned observer can realize $Z_{m1} \to x_m, Z_{m2} \to \dot{x_m}, Z_{m3} \to f$.

The motor tracking error e_{m1} , motor speed error e_{m2} and the motor control signal x_{m0} are given by

$$\begin{cases} e_{m1} = x_{mr} - Z_{m1} \\ e_{m2} = \dot{x}_{mr} - Z_{m2} \\ x_{m0} = K_{m1}e_{m1} + K_{m2}e_{m2} \end{cases} \tag{9}$$

Where K_{m1}, K_{m2} are the gains of the controller, and they are chosen as $K_{m1} = \omega_{mc}^2, K_{m2} = 2\omega_{mc}$, ω_{mc} is the bandwidth of the controller.

3.2. Load position controller design

In order to online estimate and compensate the disturbance, the load position state observer is designed, which uses the LESO to evaluate the load position Z_{l1} , load speed Z_{l2} , the disturbance of the load position loop Z_{l3} ,

$$\begin{cases} \dot{Z}_{l1} = Z_{l2} + \beta_{l1}(x_l - Z_{l1}) \\ \dot{Z}_{l2} = Z_{l3} + \beta_{l2}(x_l - Z_{l1}) + b_{l0}x_m \\ \dot{Z}_{l3} = \beta_{l3}(x_l - Z_{l1}) \end{cases} \tag{10}$$

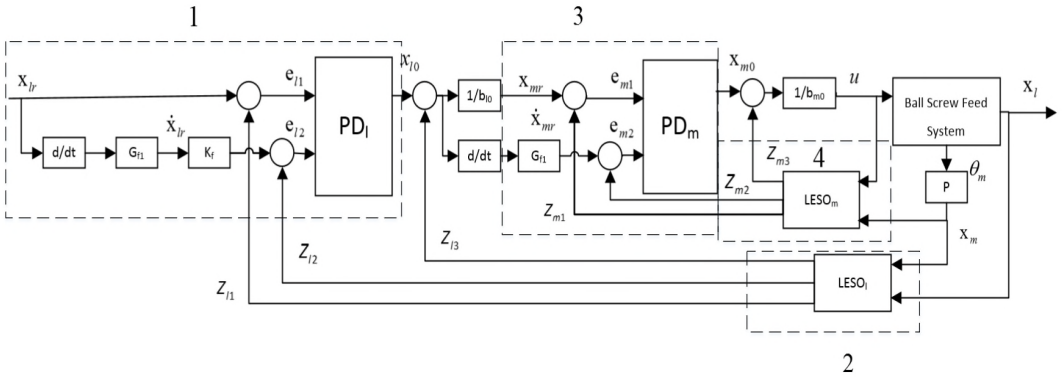

Figure 2. Block diagram of proposed controller.

Where b_{l0} is the control gain in load position loop, β_{l1}, β_{l2}, β_{l3} represent the gains of the observer. And the gains can be chosen as $\beta_{l1} = 3\omega_{l0}$, $\beta_{l2} = 3\omega_{l0}^2$, $\beta_{l3} = \omega_{l0}^3$. when it is well-tuned, $Z_{l1} \to x_l, Z_{l2} \to \dot{x}_l, Z_{l3} \to f$ can be realized.

The load tracking error e_{l1} , load speed error e_{l2} and the load control signal x_{l0} are given by

$$\begin{cases} e_{l1} = x_{lr} - Z_{l1} \\ e_{l2} = \dot{x}_{lr} - Z_{l2} \\ x_{l0} = K_{l1}e_{l1} + K_{l2}e_{l2} \end{cases} \tag{11}$$

Where K_{l1}, K_{l2} are the gains of the controller, and they are chosen as $K_{l1} = \omega_{lc}^2, K_{l2} = 2\omega_{lc}$, ω_{lc} is the bandwidth of the controller. Moreover, through differential processing, low-pass filter and proportional element, the speed feedforward compensation is generated from the load position command signal.

4. Simulated and experimental results

The cascade P-PI controller is shown in Figure 3, which was compared with proposed controller. Simulations and experiments were carried out to compare the control performance of both controllers. The main parameters of the simulation feed system are shown in the Table 1. For the cascade controller, the proportional gain of the position loop is $k_{p0} = 75$, the proportional gain and integral gain of the speed loop are $k_{pv} = 0.776, k_{iv} = 60$. For the proposed controller, the parameters of the inner loop are chosen as $\omega_{mc} = 400\pi, \omega_{mo} = 3\omega_{mc}$, while the parameters of the outer loop are chosen as $\omega_{lc} = 200\pi, \omega_{lo} = 3\omega_{lc}$.

First of all, the tracking error is compared between the two controllers. The reference trajectory is shown in Figure 4, which includes displacement, speed, acceleration and jerk. The tracking error between actual position and reference position is shown in Figure 5. It can be seen that the maximum tracking error of the proposed controller and the cascade P-PI controller are 3.9 μm and 6.8 μm respectively. In addition, Figure 6 shows the tracking errors of the two controllers when a $1\ \mathrm{N \cdot m}$ external disturbance is applied at 2.58 s. It can be seen that the proposed controller has the better ability of disturbance rejection.

In order to demonstrate the effectiveness of the controller, experimental results have also been performed. The experimental setup is shown in Figure 7. The Kollmorgen motor is operated in torque mode control, and is connected to the ball screw by coupling, both of the motor and ball screw are supported by angular contact ball bearings. The hydrostatic guideway is applied to decrease friction. A Renishaw angle encoder and a Heidenhain ultra-high precision linear encoder are used to acquire the feedback of the position. The motion command begins from the PC, through the Googol controller and Kollmorgen amplifier, to the servomotor. It can be seen in Figure 8 that the maximum tracking error of the proposed controller and the cascade P-PI controller are 4.8 μm and 7.3 μm respectively. It indicates the proposed controller has better performance than the cascade controller.

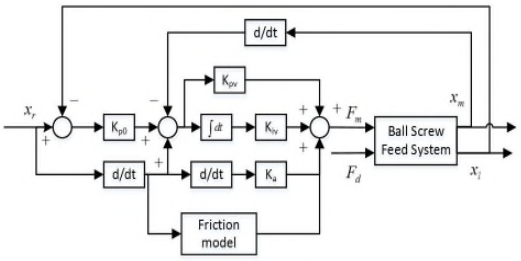

Figure 3. Model of P-PI control.

Table 1. Main parameters used in the simulation.

Parameter	Description
Moment of inertia of the motor	$20.5 \times 10^{-4}\ kg \cdot m^2$
Moment of inertia of the lead screw	$23.52 \times 10^{-4}\ kg \cdot m^2$
Mass of the worktable	$250\ kg$
Screw lead	12 mm
Equivalent torsional stiffness	$372\ \mathrm{N \cdot m}/rad$
Equivalent torsional damping	$0.15\ \mathrm{N \cdot m \cdot s}/rad$

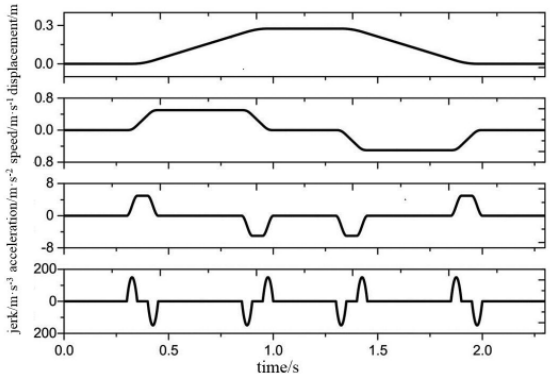

Figure 4. Reference trajectory.

5. Conclusions

An active-disturbance-rejection controller for dual position loops control was designed and applied to a ball screw feed-drive system. In order to achieve a good tracking performance, this controller combines the disturbance-rejection tracking control with PID control. Both of the loops have the state observer and position controller. The linear extended state observer was applied to online estimate and compensate the total disturbance, including parameter perturbations,

unmodeled dynamics and other disturbances, to obtain higher disturbance rejection ability. In order to obtain a better control bandwidth, the linear feedback rate of the position controller is decided by position error and speed error. Simulative and experimental results have demonstrated that the proposed controller has better tracking performance and disturbance rejection ability than traditional cascade controller.

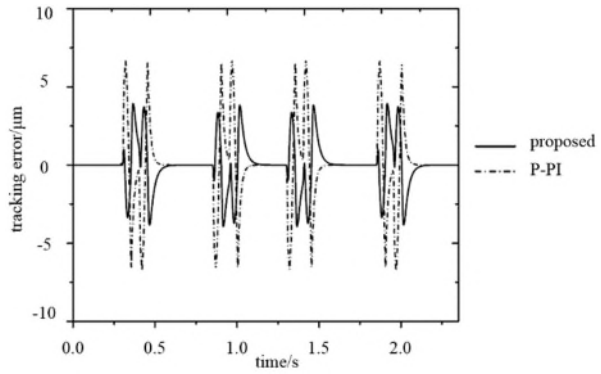

Figure 5. Tracking errors of proposed controller and P-PI controller.

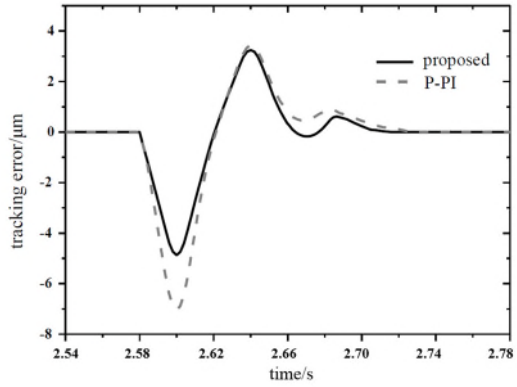

Figure 6. Tracking errors when a $1\ \mathrm{N}\cdot\mathrm{m}$ externa disturbance is applied.

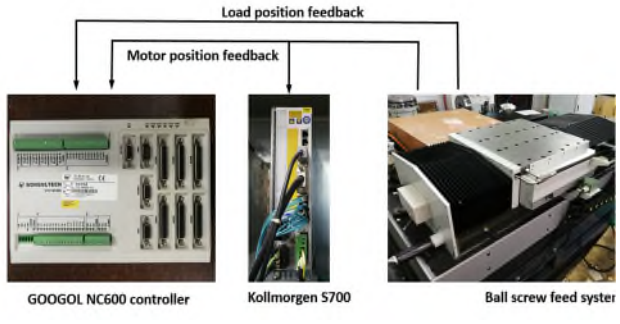

Figure 7. Feed system experimental setup.

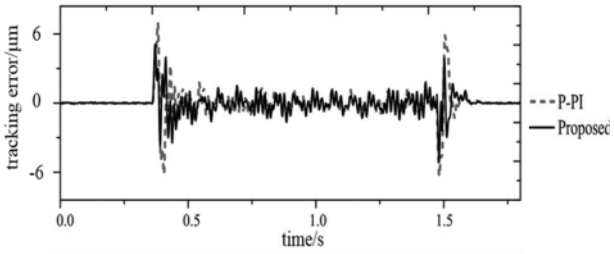

Figure 8. Experimental tracking error.

6. Funding

This work was financially supported by National Science and Technology Major Project of China (2015ZX04001002).

References

[1] Sepasi D, Nagamune R and Sassani F 2011 Tracking control of flexible ball screw drives with runout effect and mass variation *IEEE Trans. Ind. Electron.* **59** 1248-56

[2] Okwudire C and Altintas Y 2009 Minimum tracking error control of flexible ball screw drives using a discrete-time sliding mode controller *J. Dyn. Syst. Meas. Contr.* **131** 545-53

[3] Vicente D A, Hecker R L, Villegas F J and Flores G M 2012 Modeling and vibration mode analysis of a ball screw drive *Int. J. Adv. Manu. Technol.* **58** 257-65

[4] Dong L and Tang W 2014 Control of ball screw drives using adaptive backstepping sliding mode controller and minimum tracking error prefilter *IEEE Int. Conf. Contr. Autom.*

[5] Ohnishi K 1987 A new servo method in mechatronics *Trans. Jpn. Soc. Elect. Eng.* **107** 83–6

[6] Elfizy A, Bone G and Elbestawi M 2004 Model-based controller design for machine tool direct feed drives *Int. J. Mach. Tools Manu.* **44** 465-77

[7] Yan M and Shiu Y 2008 Theory and application of a combined feedback-feedforward control and disturbance observer in linear motor drive wire-EDM machines *Int. J. Mach. Tools Manu.* **48** 388-401

[8] Huang W S, Liu C W, Hsu P L and Yeh S S 2009 Precision control and compensation of servomotors and machine tools via the disturbance observer *IEEE Trans. Ind. Electron.* **57** 420-9

[9] Huang C E, Li D and Xue Y 2013 Active disturbance rejection control for the ALSTOM gasifier benchmark problem *Contr. Eng. Pract.* **21** 556-64

[10] Okwudire C and Altintas Y 2009 Minimum tracking error control of flexible ball screw drives using a discrete-time sliding mode controller *J. Dyn. Syst. Meas. Contr.* **131** 545-53

[11] Pan H, Sun W, Gao H, Hayat T and Alsaadi F 2015 Nonlinear tracking control based on extended state observer for vehicle active suspensions with performance constraints *Mechatronics* **30** 363-70

[12] Kempf C J and Kobayashi S 1999 Disturbance observer and feedforward design for a high-speed direct-drive positioning table *IEEE Trans. Contr. Syst. Technol.* **7** 513-26

[13] Cui R, Chen L, Yang C and Chen M 2017 Extended state observer-based integral sliding mode control for an underwater robot with unknown disturbances and uncertain nonlinearities *IEEE Trans. Ind. Electron.* **64** 6785-95

[14] Liu J, Vazquez S, Wu L, Marquez A and Gao H 2017 Extended state observer-based sliding-mode control for three-phase power converters *IEEE Trans. Ind. Electron.* **64** 22-31

[15] Zhang C and Chen Y 2017 Adaptive tracking control of ball screw drives with load mass variations *J. Syst. Contr. Eng.* **231** 693–701

[16] Sun W, Pan H, Zhang Y and Gao H 2014 Multi-objective control for uncertain nonlinear active suspension systems *Mechatronics* **24** 318-27

[17] Li S and Liu Z 2009 Adaptive speed control for permanent-magnet synchronous motor system with variations of load inertia *IEEE Trans. Ind. Electron.* **56** 3050-9

[18] Jin J, Wang S and Huang S 2014 Adaptive disturbance observer design for servo drive system with time-varying load inertia *IEEE Int. Conf. Mechatronics Autom*.

[19] Su J, Qiu W, Ma H and Peng Y 2004 Calibration-free robotic eye-hand coordination based on an auto disturbance-rejection controller *IEEE Trans. Rob.* **20** 899-907

[20] Zheng Q and Dong L 2007 A disturbance rejection based control system design for Z-axis vibratory rate gyroscopes *IEEE Int. Conf. Contr. Autom.* **222** 23-30

[21] Pan Y, Shih Y, Horng R and Lee A 2009 Advanced parameter identification for a linear-motor-driven motion system using disturbance observer *Int. J. Precis. Eng. Man.* **10** 35-47

[22] Yao J, Jiao Z and Ma D 2014 Adaptive robust control of DC motors with extended state observer *IEEE Trans. Ind. Electron.* **61** 3630-7